14 April 2000

Chemical Physics Letters 320 (2000) 639–644

CHEMICAL PHYSICS LETTERS

www.elsevier.nl/locate/cplett

New photon upconversion processes in Yb^{3+} doped $CsMnCl_3$ and $RbMnCl_3$

Rafael Valiente, Oliver Wenger, Hans U. Güdel *

Department of Chemistry and Biochemistry, University of Bern, Freiestrasse 3, CH-3000 Bern 9, Switzerland

Received 4 February 2000

Abstract

Excitation around 980 nm and 935 nm leads to visible luminescence in the title compounds below 100 K. The broad luminescence band centered around 690 nm and 630 nm in Yb^{3+} doped $CsMnCl_3$ and $RbMnCl_3$, respectively, is identified as a $^4T_1 \rightarrow {}^6A_1$ transition on Mn^{2+}. The upconversion excitation spectrum follows the $^2F_{7/2} \rightarrow {}^2F_{5/2}$ absorptions around 980 nm and 935 nm. Excitation with 10 ns pulses induces instantaneous upconversion luminescence, indicating that no energy transfer is involved in the process. The most likely mechanism for this new type of upconversion process is based on exchange interactions between neighboring Yb^{3+} and Mn^{2+} ions. In a dimer picture the intermediate excitation is mainly, but not exclusively localized on Yb^{3+}, whereas the upper emitting state is mainly but not exclusively localized on Mn^{2+}.

1. Introduction

One way to convert near-infrared (NIR) radiation into visible (VIS) light is by a so-called upconversion (UC) process. A number of UC mechanisms have been established and described [1]. Typically, those involving energy transfer (ET) steps can be identified by a rise and decay of their transients after a pulsed excitation [2]. Those involving a sequence of ground-state absorption (GSA) and excited-state absorption (ESA) steps, on the other hand, exhibit an instantaneous rise of the UC luminescence by an excitation pulse [2].

The presence of more than one metastable excited state is a requirement for upconversion to occur. The first step is always a GSA to an intermediate level, in our case in the NIR, followed by one or more ESA or ET processes to produce VIS luminescence. UC is best established in lanthanide compounds, because they often have metastable excited f–f states. We have recently shown that UC can also be induced in some selected transition metal ion doped crystals. The ions, Ti^{2+} [3], Ni^{2+} [4], Mo^{3+} [5], Re^{4+} [6] and Os^{4+} [7] in halide lattices have more than one metastable excited state, and the same principles as in lanthanide systems are valid.

In the present Letter we show that a new and very efficient type of UC process can be induced by a proper combination of transition metal and lanthanide ions in a crystal lattice. The $CsMnCl_3$ and $RbMnCl_3$ compounds are known to show VIS

* Corresponding author. Fax: +41-31-631-4399; e-mail: guedel@iac.unibe.ch

0009-2614/00/$ - see front matter
PII: S0009-2614(00)00278-5

$^4T_1 \rightarrow {}^6A_1$ luminescence below 100 K [8]. The only f–f excitation of Yb^{3+} is $^2F_{7/2} \rightarrow {}^2F_{5/2}$ below 1 μm, and there are no excited states in the VIS that could complicate the situation. For this reason and the fact that all the f–f oscillator strength is concentrated in that one $^2F_{7/2} \rightarrow {}^2F_{5/2}$ transition, Yb^{3+} is often used as a sensitizer for UC processes in Tm^{3+} [9], Er^{3+} [10], Ho^{3+} [11] and Pr^{3+} [12] systems. We report experimental results and discuss possible mechanisms for the new NIR to VIS upconversion process.

2. Experimental

Single crystals of Yb^{3+} doped $CsMnCl_3$ and $RbMnCl_3$ were grown by the Bridgman technique using stoichiometric amounts of CsCl, RbCl and $MnCl_2$ and a trace of $YbCl_3$. The estimated molar concentration of Yb^{3+} is 0.1% and 0.9% in the $RbMnCl_3$ and $CsMnCl_3$ crystals, respectively. Polarized absorption spectra were measured on a Cary 5E spectrometer with $\boldsymbol{E} \| \boldsymbol{c}$ (π) and $\boldsymbol{E} \perp \boldsymbol{c}$ (σ).

Upconversion luminescence was excited by an Ar^+ laser (Spectra Physics 2060-10 SA) pumped tunable Ti:sapphire laser (Spectra Physics 3900S). The emission was dispersed by a 0.85 m double monochromator (Spex 1402) and detected by a cooled photomultiplier (Hamamatsu 3310-01) using a photon counting system (Standford Research 400). All the spectra were corrected for the sensitivity of the detection system and for the refractive index of air (vacuum correction). They are represented as number of photons versus wavenumbers.

For pulsed excitation experiments the output of a Nd:YAG laser (Quanta Ray DCR 3) pumped dye laser (Lambda Physik FL3002) was Raman shifted (Quanta Ray, RS-1, H_2, 340 psi) using pyridine 1 to cover the range 935–1035 nm. The sample luminescence was dispersed by a 0.75 m single monochromator (Spex 1702) equipped with a 600 grooves/mm grating. For the time-resolved detection a multichannel scaler (Standford Research SR430) was used.

The crystal was cooled by a quartz flow tube in the 10–120 K temperature range for luminescence measurements and a closed-cycle cryostat (Air Products) for absorption experiments (10–300 K).

3. Results

Both Yb^{3+} doped $CsMnCl_3$ and $RbMnCl_3$ show a typical $^4T_1 \rightarrow {}^6A_1$ broad band Mn^{2+} emission after $^2F_{7/2} \rightarrow {}^2F_{5/2}$ excitation around 980 nm and 935 nm. Experimental results obtained at 10 K are shown in Fig. 1. There is no difference to the luminescence spectra obtained by direct Mn^{2+} excitation with an Ar^+ laser at the same temperature. The luminescence is quenched above 200 K and 100 K in $CsMnCl_3$:Yb^{3+} and $RbMnCl_3$:Yb^{3+}, respectively. But this quenching is an intrinsic property of the manganese systems and occurs independently of the mode of excitation. For $CsMnCl_3$:Yb^{3+}, the 10 K NIR excitation spectrum of the VIS luminescence exactly corresponds to the 10 K absorption spectrum of Yb^{3+} between 930 nm and 980 nm. This is shown in Fig. 2. Whereas the band energies in the two spectra are exactly the same, their relative intensities are not. This will be explained in Section 4. For $RbMnCl_3$:Yb^{3+} the situation is slightly more complicated: the absorption spectrum shows the presence of inequivalent Yb^{3+} sites. Independent experiments with selective excitation show that at 10 K in our very diluted crystal energy transfer between these sites is negligible. The UC excitation spectra show that the dominant contribution to the upconversion is due to only one of the inequivalent sites. The 10 K absorption and excitation spectra in Fig. 2 measured with high resolution show that three crys-

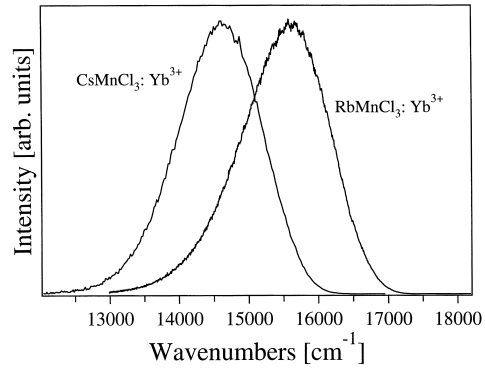

Fig. 1. 10 K upconversion luminescence spectra of $CsMnCl_3$:Yb^{3+} and $RbMnCl_3$:Yb^{3+} excited at 10 680 cm^{-1} and 10 688 cm^{-1}, respectively.

tal-field components A, B and C of the $^2F_{7/2} \rightarrow {}^2F_{5/2}$ excitation of Yb^{3+} exhibit some additional splittings. We ascribe these splittings to the fact that the host lattice $CsMnCl_3$ is magnetically ordered at 10 K ($T_N = 67$ K) and thus the Yb^{3+} ions are exposed to a molecular field [13].

By simultaneously measuring the Mn^{2+} luminescence in the VIS and the $^2F_{5/2} \rightarrow {}^2F_{7/2}$ luminescence of Yb^{3+} in the NIR at 10 K, we determined the ratio of Yb^{3+} excitations leading to UC. This ratio is of course dependent on the laser power, and for a power of 120 mW focused with a 50 mm focal lens onto the Rb and Cs crystals, respectively, we obtained the followings ratios of VIS/NIR photons: 12/100 for $RbMnCl_3$:Yb^{3+} and 45/100 for $CsMnCl_3$:Yb^{3+}.

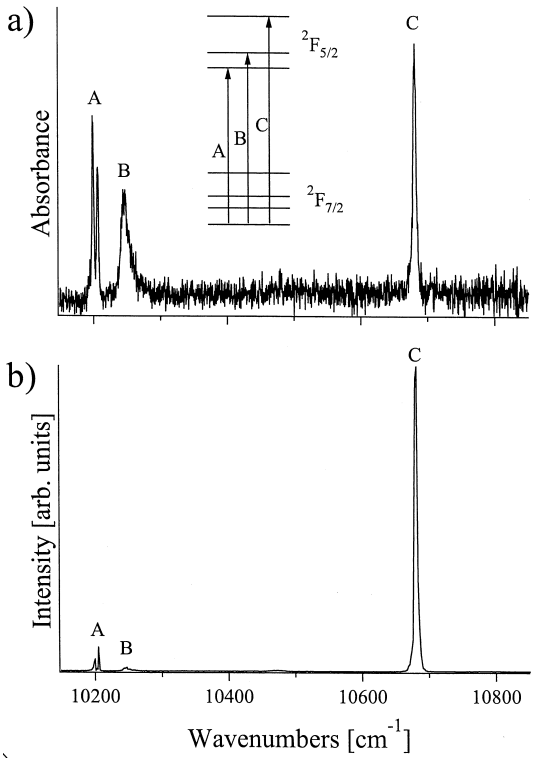

Fig. 2. High-resolution absorption (a) and upconversion excitation spectra (b, luminescence monitored at 15 800 cm^{-1}) of $CsMnCl_3$:Yb^{3+} at 10 K. The excitation spectrum is corrected for the decreasing Ti:sapphire laser output towards smaller energy. The assignment of the three main bands A, B and C to the three crystal-field components is shown in the scheme.

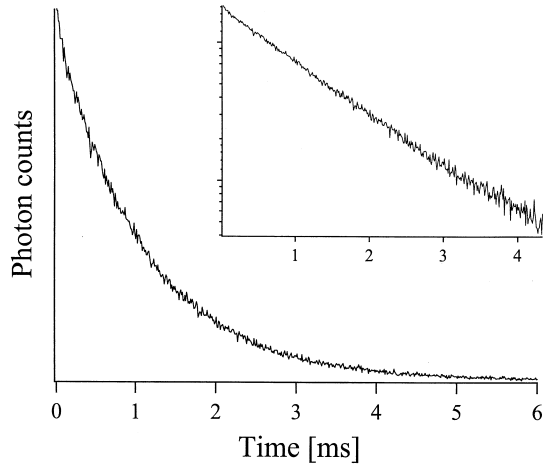

Fig. 3. Time evolution at 10 K of the upconverted luminescence intensity of $RbMnCl_3$:Yb^{3+} (observed at 15 750 cm^{-1}) after a 10 ns pulsed excitation at 10 688 cm^{-1}. The inset shows the same data in a semilog representation.

Fig. 3 shows the time dependence of the 10 K Mn^{2+} luminescence intensity at 15 750 cm^{-1} from $RbMnCl_3$:Yb^{3+} after 10 ns pulsed Yb^{3+} excitation at 10 688 cm^{-1}. It shows a perfectly exponential decay and, more importantly, it does not show any rise. This is relevant for an identification of the upconversion mechanism, as will be shown in Section 4.

4. Discussion

A Mn^{2+} emission induced by upconversion is a remarkable observation by itself, and it has no precedent. Our experiments clearly demonstrate that the Yb^{3+} ions are participating. The process is thus identified as a cooperative process involving both Yb^{3+} and Mn^{2+}. The fact that upon Yb^{3+} excitation upconversion yields of 40 percent or more can be achieved, is another surprise. It reveals a potentially very efficient UC mechanism, which apparently has not been explored and exploited so far. In order to get an understanding of the mechanism behind our observations we examine the crystal lattices of $CsMnCl_3$ and $RbMnCl_3$ and search the literature for cooperative processes in coupled transition metal and lanthanide systems.

$CsMnCl_3$ and $RbMnCl_3$ crystallize in the trigonal (space group R3m) [14] and hexagonal (space group $P6_3/mmc$) [15] systems, respectively, and order antiferromagnetically at $T_N = 67$ K and 94 K, respectively [13]. They represent intermediate structure types between the $CsNiCl_3$ and $KNiF_3$ perovskite structures. Whereas $CsNiCl_3$ contains $NiCl_3^-$ chains built up of face-sharing octahedra, all the octahedra share corners in the cubic $KNiF_3$ structure. Fig. 4, which shows the relevant fragments of the $CsMnCl_3$ and $RbMnCl_3$ structures, illustrates that both face and corner sharing occur, with corner sharing dominating in $RbMnCl_3$. Exchange interactions between neighboring Mn^{2+} ions, which eventually lead to the magnetic order, occur by both pathways. In both structures there are two crystallographically nonequivalent Mn^{2+} sites, one with D_{3d} (site A in Fig. 4) and one with C_{3v} (site B in Fig. 4) point symmetry. Since the $^2F_{7/2} \rightarrow {}^2F_{5/2}$ excitations in Fig. 2 are dominated by electronic origins and the same is true in the $RbMnCl_3$:Yb^{3+} spectrum, the Yb^{3+} ions most likely substitute the C_{3v} sites in both crystals. Charge compensation most likely occurs by a Mn^{2+} vacancy adjacent to two Yb^{3+} ions or an Yb^{3+} and an impurity Mn^{3+} ion. Both lattices offer two such possibilities, of which only one is used in $CsMnCl_3$:Yb^{3+}, but in $RbMnCl_3$:Yb^{3+} inequivalent Yb^{3+}-vacancy arrangements are realized. In both crystals the upconversion process is dominated by only one Yb^{3+} site. We are engaged in further work to determine whether the relevant Yb^{3+}–Mn^{2+} pair is face or corner sharing.

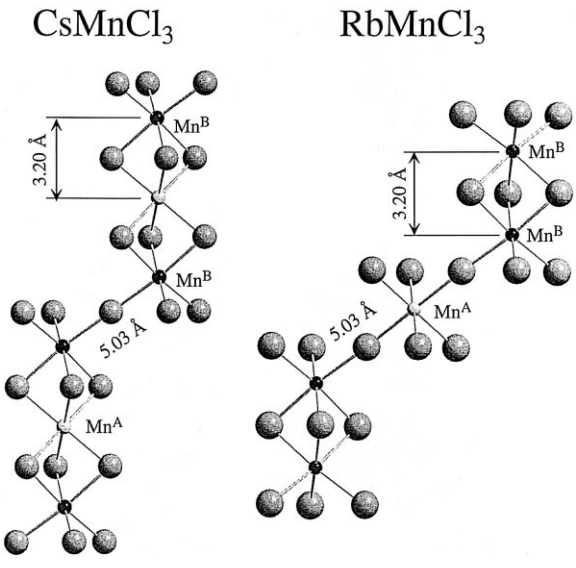

Fig. 4. Relevant elements of the $CsMnCl_3$ and $RbMnCl_3$ crystal structures illustrating the two types of Mn sites, D_{3d} (Mn^A) and C_{3v} (Mn^B) and bridging arrangements (face and corner sharing octahedra).

Yb^{3+} is known to be an excellent upconversion sensitizer for ions such as Tm^{3+}, Er^{3+}, Ho^{3+} and Pr^{3+} [9–12]. All these ions have intermediate excited states slightly below 10 200 cm^{-1}, so that the initial $^2F_{7/2} \rightarrow {}^2F_{5/2}$ excitation of Yb^{3+} is efficiently transferred. We are facing a physically completely different situation. There is no excited state of Mn^{2+} around 10 000 cm^{-1}, so that the excited Yb^{3+} is directly involved in the UC process. There is some analogy to Yb^{3+} and Tb^{3+} codoped CaF_2, SrF_2 [16] and YF_3 [17], which exhibit VIS Tb^{3+} emission after Yb^{3+} excitation below 1 μm. The following two mechanisms have been mainly discussed to account for this phenomenon: (i) Two excited Yb^{3+} ions simultaneously transfer their energy to a near-by Tb^{3+} ion [16,17]; (ii) simultaneous photon absorption and $Yb^{3+} \rightarrow Tb^{3+}$ energy transfer mediated by multipole–multipole interactions [18]. We can rule out mechanism (i) for our Yb^{3+} doped Mn^{2+} lattice on the basis of the observed time dependence after a short excitation pulse, see Fig. 3. Since the transient shows no rise the mechanism cannot involve an energy transfer step. Further support for this conclusion will be provided below when we discuss the difference in the behavior between $CsMnCl_3$:Yb^{3+} and $RbMnCl_3$:Yb^{3+}. We also believe that a multipole interaction mechanism as proposed in Ref. [18] is unlikely in our systems. The main reason is the high efficiency of the process in $CsMnCl_3$:Yb^{3+} and its site selectivity in $RbMnCl_3$:Yb^{3+}.

These observations all point to an exchange mechanism. Tanabe and coworkers have proposed an intensity mechanism for transitions in exchange coupled dimers and extended systems [19]. There is plenty of experimental evidence for the efficiency of this mechanism in exchange coupled transition metal ion systems. Cooperative transitions in lanthanide systems, on the other hand, have usually been interpreted in terms of multipolar interactions. A convincing example of an efficient Tanabe mechanism in a

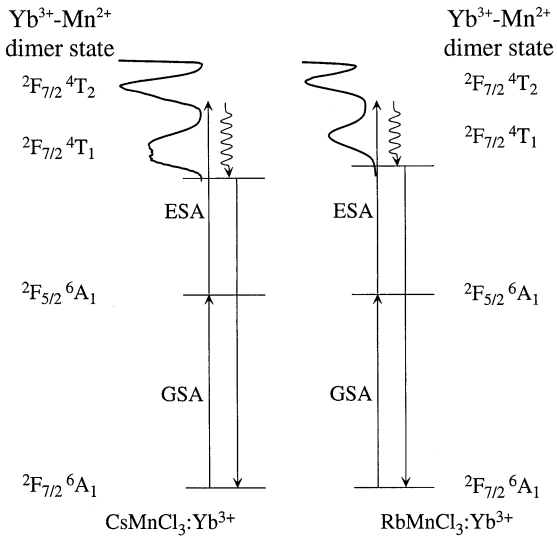

Fig. 5. Schematic representation of the upconversion processes in the two systems with the onset of the 10 K absorption spectra of $CsMnCl_3$ and $RbMnCl_3$ at the top. The designation of states is in Yb^{3+}–Mn^{2+} dimer notation. Straight arrows correspond to radiative, curly arrows to multiphonon relaxation processes.

mixed transition metal/lanthanide system are the dominant cooperative absorption and luminescence transitions in Cr^{3+} doped $EuAlO_3$ [20]. The R-lines corresponding to the $^4A_2 \leftrightarrow {}^2E$ transitions in Cr^{3+} are very weak compared to the sidebands corresponding to cooperative transitions in which a neighboring Eu^{3+} ion is simultaneously excited from $^7F_0$ to $^7F_1$. Thus a large transition dipole moment is induced by the Tanabe mechanism in a Cr^{3+}–Eu^{3+} pair for a transition between the $^7F_1$ excited state of Eu^{3+} and the ^2E excited state of Cr^{3+}. Using the same mechanism we can now account for the upconversion processes in Yb^{3+} doped $CsMnCl_3$ and $RbMnCl_3$. Based on an Yb^{3+}–Mn^{2+} dimer picture this is illustrated in Fig. 5. The dimer ground state is represented by $|^2F_{7/2}\,{}^6A_1\rangle$, the intermediate excited state in the NIR by $|^2F_{5/2}\,{}^6A_1\rangle$ and the relevant higher excited states by $|^2F_{7/2}\,{}^4T_1\rangle$ and $|^2F_{7/2}\,{}^4T_2\rangle$. The GSA step to the intermediate state is exchange enhanced and thus more efficient than in a Yb^{3+} single ion. The ESA step $|^2F_{5/2}\,{}^6A_1\rangle \rightarrow |^2F_{7/2}\,{}^4T_1\rangle$ or $|^2F_{7/2}\,{}^4T_2\rangle$ is made possible and gains intensity by the same Tanabe exchange mechanism. By a slight mixing of wavefunctions the intermediate state is essentially but not exclusively localized on Yb^{3+} and, analogously, the emitting state is essentially but not exclusively localized on Mn^{2+}. Fig. 5 also explains the observed difference in the efficiency of the UC process in the two crystals using excitation energy around 10 685 cm^{-1}. Due to a difference in the absorption spectrum the ESA step is much more efficient in $CsMnCl_3$:Yb^{3+}, because it hits the rising slope of the $^4T_2$ absorption band, whereas in $RbMnCl_3$:Yb^{3+} the ESA cross-section is very small, because it only hits the far tail of the $^4T_1$ absorption. In the steep slope the ESA cross-section in $CsMnCl_3$:Yb^{3+} is strongly energy dependent, increasing with increasing the energy. This is the reason for the different relative intensities in the two spectra of Fig. 2.

In conclusion, we have demonstrated a new type of NIR to VIS upconversion process by combining Yb^{3+} and Mn^{2+} in a crystal lattice. We are in the process of studying the underlying mechanisms in detail. We also believe that the same principle can be used to create other combinations of ions, which should be able to convert NIR radiation into visible light.

Acknowledgements

We are indebted to Daniel Gamelin and Markus Wermuth for fruitful discussions. This work was financially supported by the Swiss National Science Foundation.

References

[1] F. Auzel, Proc. IEEE 61 (1973) 758.
[2] P. Müller, M. Wermuth, H.U. Güdel, Chem. Phys. Lett. 290 (1998) 105.
[3] S.M. Jacobsen, H.U. Güdel, J. Luminesc. 43 (1989) 125.
[4] U. Oetliker, M.J. Riley, P.S. May, H.U. Güdel, Coord. Chem. Rev. 111 (1991) 125.
[5] D.R. Gamelin, H.U. Güdel, J. Am. Chem. Soc. 120 (1998) 12143.
[6] D.R. Gamelin, H.U. Güdel, Inorg. Chem. 38 (1999) 5154.
[7] M. Wermuth, H.U. Güdel, J. Am. Chem. Soc. 121 (1999) 10102.
[8] U. Kambli, H.U. Güdel, J. Phys. C: Solid State Phys. 17 (1984) 4041.
[9] F.W. Ostermayer, J.P. van der Ziel, H.M. Marcos, L.G. van Uitert, J.E. Geusic, Phys. Rev. B 3 (1971) 2698.

[10] M.F. Auzel, C.R. Acad. Sci. (Paris) 262 (1966) 1016.
[11] R.K. Watts, H.J. Richter, Phys. Rev. B 6 (1972) 1584.
[12] B. Jaquier, C. Linares, R. Mahioou, J.L. Adam, E. Denoue, J. Lucas, J. Luminesc. 60 and 61 (1997) 175.
[13] M. Melamud, J. Makovsky, H. Shaked, Phys. Rev. B: Condensed Matter 3 (1971) 3873.
[14] J. Goodyear, D.J. Kennedy, Acta Cryst. B 29 (1973) 744.
[15] J. Goodyear, G. Steigmann, E. Ali, Acta Cryst. B 33 (1977) 256.
[16] L.D. Livanova, I.G. Saitkulov, A.L. Stolov, Soviet Phys.-Solid State 11 (1969) 750.
[17] F.W. Ostermayer, L.G. van Uitert, Phys. Rev. B 1 (1970) 4208.
[18] M. Altarelli, D.L. Dexter, Optics Commun. 2 (1970) 36.
[19] J. Ferguson, H.J. Guggenheim, Y. Tanabe, J. Phys. Soc. Jpn. 21 (1966) 692.
[20] J.P. van der Ziel, L.G. van Uitert, Phys. Rev. 180 (1969) 343.